Quantum Annealing for SAR System Design and Processing

Sigurd Huber, Kay Glatting, Gerhard Krieger, and Alberto Moreira
Microwaves and Radar Institute, German Aerospace Center (DLR), Oberpfaffenhofen, Germany

https://ieeexplore.ieee.org/document/9944345

Abstract

In the last two decades synthetic aperture radar (SAR) systems for Earth observation have undergone rapid evolution in terms of mapping capability and system complexity. Numerous optimization and processing tasks are related to these kind of systems or the evaluation of SAR data. Usually, these problems are solved with the aid of conventional digital computers. However, with the emergence of quantum computers, many of these tasks may have the potential to be solved faster, to be solved with higher precision or to be solvable at all on these machines. Here, we present the conceptual idea of quantum annealing, a specific implementation of quantum computing and apply a real quantum annealer, developed and operated by D-Wave Systems Inc., to two dedicated optimization problems in the field of synthetic aperture radar.

1 Introduction

In modern SAR system design and SAR signal processing there are a wide variety of problems, which may only be solved suboptimal on conventional digital computers. Examples are the optimization of the phase excitation coefficients for the suppression of ambiguities in future SAR systems [12, 13], the optimization of SAR antenna geometries, the resolution of phase ambiguities in SAR interferometry (phase unwrapping), machine learning for feature extraction in SAR imagery or the processing of SAR raw data.

Recently, rapid progress in the field of quantum computing has been achieved. There are two major branches in quantum computation: One are gate-based quantum computers who, similar to classical computers, are constructed from logical gates, so called quantum gates. These quantum computing architectures, currently, implement in the order of five to 50 fully entangled qubits. A second development in quantum computers are so called quantum annealers, which rest upon the quantum adiabatic theorem. Adiabatic quantum computation is universal, as gate-based quantum computation, but its specific implementation as quantum annealer is especially powerful, when it comes to all kinds of combinatoric optimizations problems.

Quantum computers will not in general replace classical computers in the foreseeable future. In the coming years quantum computers will be made accessible via cloud services and eventually support computations locally by a quantum processing unit (QPU), similar to co-processors like graphical processing units (GPUs) in conventional workstations. In order to be prepared for these highly dynamical developments in the field of quantum computing, a first step in this paper shall be made to explore the potential of existing and in the near-future available quantum computers for SAR applications. Here, we present two simple examples in the context of SAR [11, 13, 16], which demonstrate the concepts of problem formulation and solution capabilities of a quantum annealing system, developed and operated by D-Wave Systems Inc.

2 Quantum Annealing in a Nutshell

Quantum annealing is a specific implementation of quantum computation. It relies on the quantum adiabatic theorem [4], which states that if a physical system is initially in a certain quantum state and changes sufficiently slowly under a small perturbation, it will remain in this state, even if the associated energies of the initial and final states are different. This principle has first been exploited for classical combinatorial optimization problems [2]. The idea is to encode the solution to a problem in the ground state of a physical system - the quantum computer - represented by its Hamiltonian H

$$H(t) = A(t)H_\mathrm{i} + B(t)H_\mathrm{f}\,, \quad t \in [0,T]\,, \tag{1}$$

where A and B are scalar functions. $H(t)$ governs the dynamics of the system described by the time-dependent Schrödinger equation

$$H(t)\,|\Psi(t)\rangle = \mathrm{i}\hbar\partial_t\,|\Psi(t)\rangle\,, \tag{2}$$

with $\hbar$ the reduced Planck constant $h/(2\pi)$ and $|\Psi(t)\rangle$ an arbitrary state of the system. The quantum computational Hamiltonian is prepared in the ground state $|e_0(t=0)\rangle$ at the beginning of the annealing cycle, with its corresponding initial Hamiltonian H_i and changed slowly towards its final Hamiltonian H_f, representing the computational problem to be solved. In the simplest case the time dependent functions $A(t)$ and $B(t)$ may describe linear control functions such as $A(t) = 1 - t/T$ and $B(t) = t/T$ [8], where T is the annealing time or run time of the algorithm. However, in real quantum computers $A(t)$ and $B(t)$ are usually non-linear as in D-Wave's Quantum Annealer [7]. The instantaneous eigenstates $|e_\mu(t)\rangle$ and eigenenergies $e_\mu(t)$ as solution of

$$H(t)\,|e_\mu(t)\rangle = e_\mu(t)\,|e_\mu(t)\rangle\,, \tag{3}$$

encode, at the end of the annealing cycle at $t = T$, the problem solution. The task of choosing the annealing time T is not an easy one, since it depends on the energy difference Δ of the two lowest eigenenergies

$$\Delta = \min_{0 \le t \le T} \{e_1(t) - e_0(t)\} \, . \tag{4}$$

Clearly, this energy difference is not known a priori and therefore has to be chosen heuristically, except maybe for simple Hamiltonians. Typical run times are in the range [2]

$$T \sim O(1/\Delta^3) \cdots O(1/\Delta^2) \, . \tag{5}$$

At this point it should be mentioned that the question if a quantum adiabatic algorithm offers a speedup over the fastest classical solution, is not settled yet. Another way to express the cost for the execution of an adiabatic algorithm is the quantity [1]

$$T \max_t \|H(t)\| \, , \tag{6}$$

which could be equated with the number of gates of a standard gate-based quantum computer. Here, $\|.\|$ denotes the operator norm [2].

A specific class of Hamiltonians allows solving binary quadratic optimization problems. In the so called Ising Spin glass model the final Hamiltonian takes the form [10, 5, 7]

$$H_\mathrm{f} \sim \sum_i h_i \sigma_z^{(i)} + \sum_{i,j>i} J_{ij} \sigma_z^{(i)} \sigma_z^{(j)} \, , \tag{7}$$

where (h_i, J_{ij}) represent the problem parameters and $\sigma_z^{(i)}$ denote Pauli matrices acting on the ith qubit. In the following, for the mathematical treatment of the problem, it is convenient to replace the notation with spin-states by binary variables $\sigma_z^{(i)} \mapsto x_i \in [0,1]$.

In this work we look at the principal capability of a quantum computer to solve problems in the field of array processing. This means, we compare the solutions found by a quantum computer with the optimal solution generated by a classical computer, in case of small problem sizes. In a second example, the quantum solution is compared to the analytic solution.

3 Array Processing Problems

Array processing [18, 21] is a subject in the field of signal processing. Obviously, as a consequence of technological history, the signal processing methods and algorithms have been developed for classical computers. Our goal here is not to transform the array processing problem itself into the language of quantum physics, but rather exploit quantum computers to solve specific optimization problems. Up to this date, several problems have been identified adequate for quantum computers and in particular for adiabatic quantum computation [15]. In the following we present two array processing problems relevant for SAR remote sensing, to be solved with the help of a quantum computer.

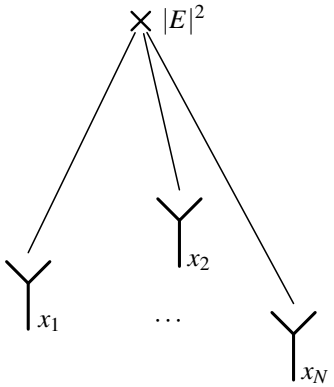

Figure 1 Example for a sparse array: Here, the optimization goal lies in the selection of a subset with a fixed number of antenna elements, such that the field is maximized at a given point in space.

3.1 Sparse Arrays

Sparse arrays or thinned arrays [6, 18], as they are called, are important for radar or communications applications, but also for advanced concepts for distributed SAR systems [14, 20, 9, 19]. The goal is to select a subset of a given set of antenna elements such that the gain in a certain direction (or multiple directions) is preserved, while discarding all redundant elements. By this it is possible to reduce the complexity and cost of an array system without sacrificing too much performance. Here, our task shall be to maximise the array gain at a certain location under the constraint of selecting exactly M out of N elements. This is a combinatorial optimization problem with $\binom{N}{M}$ solutions. The strength of a quantum computer lies in its ability that it can keep track of all 2^N array configurations by means of superposition. Such optimization problems quickly become infeasible for brute force methods and require sophisticated solution algorithms.

In our simplified example (see Fig. 1) the elements shall be represented by non-interacting point sources, with the (co-polar) electric field component E_i in frequency domain, according to

$$E = \sum_{i=1}^{N} x_i E_i \, , \quad E_i \sim E_0 \frac{\mathrm{e}^{-\mathrm{i}2\pi r_i/\lambda}}{r_i} \, , \quad x_i \in \{0,1\} \, , \tag{8}$$

where λ is the wavelength and r_i is the distance between the ith array element and the point of interest. Each array element is associated with a quantum variable x_i which can either switch an element on or off. Then the energy functional for this optimization problem can be cast in the form

$$e_\mu = -\left| \sum_{i=1}^{N} x_i E_i \right|^2 + \gamma \left(\sum_{i=1}^{N} x_i - M \right)^2 \, , \tag{9}$$

with μ as the decimal encoding of the binary string $\boldsymbol{x} \in \{0,1\}^N$, which labels the corresponding eigenstate. Here, the first term on the right side denotes the objective while the second term represents the constraint, weighted with some parameter $\gamma \in \mathbb{R}_+$. Expanding this energy function

yields

$$e_\mu = \sum_i \left(\gamma(1-2M) - |E_i|^2\right) x_i + \sum_i \sum_{j>i} 2\left(\gamma - E_i' E_j' - E_i'' E_j''\right) x_i x_j + \gamma M^2 \,, \quad (10)$$

where the electric field has been decomposed in its real and imaginary part $E_i = E_i' + \mathrm{i}E_i''$.

In order to demonstrate the capabilities of the D-Wave quantum annealer and to understand and interpret the results, a rather low number of array elements ($N = 10$, $M = 5$) has been chosen. The simulation is set up such, that these ten elements are uniformly distributed in a volume in units of λ of size $\Delta x \times \Delta y \times \Delta z = 10 \times 10 \times 2$ with a cartesian coordinate system at the center of the volume. The point of interest, where the field shall be evaluated is 5λ away from the origin in z-direction.

In a first step it is worth visualizing the energy function e_μ, as shown in Fig. 2. Here, the eigenenergies have been plotted for each point of the N-dimensional state space (Hilbert space). For example the number 370 is the decimal repre-

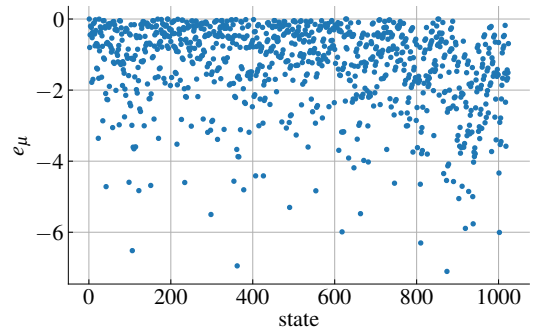

(a) $\gamma = 0$

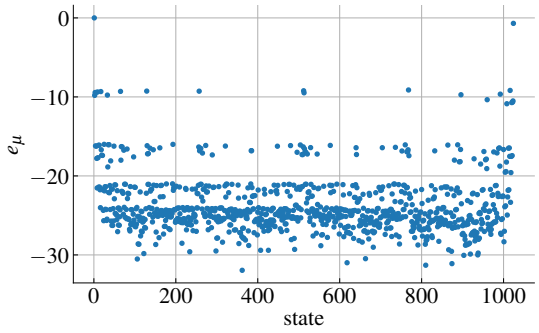

(b) $\gamma = 1$

Figure 2 Eigenenergies e_μ for all possible array configurations encoded by decimal numbers. The parameter γ controls the incorporation of the constraint (cf. equation (9)).

sentation of state $|0101110010\rangle$, where elements two, five, six, seven and nine are active. Important to mention here is that the energies should be regarded as normalized values, which have been computed from equation (10), neglecting the constant term. Figures 2a and 2b show two cases - in the first one without constraint ($\gamma = 0$) and in the second one with constraint taken into account ($\gamma = 1$). Clearly, the choice of the parameter γ affects the solution topology, where, in the first example, one deals with a 'few' pronounced minima, while in the second case the problem is transformed having many local minima close in energy level. In theory, this would affect the annealing time, which depends on the energy gap of the two lowest eigenstates according to equation (4).

The solution using D-Wave's 2000Q lower-noise system has been computed with a fixed annealing time of $T = 20\,\mu$s. This first generation quantum computer implements their so called chimera topology [5] with 2048 qubits. The problem has been submitted via a Python script to D-Wave. Figure 3 on the left shows the results for the case $\gamma = 0$ and on the right for $\gamma = 1$. The corresponding graphs shown

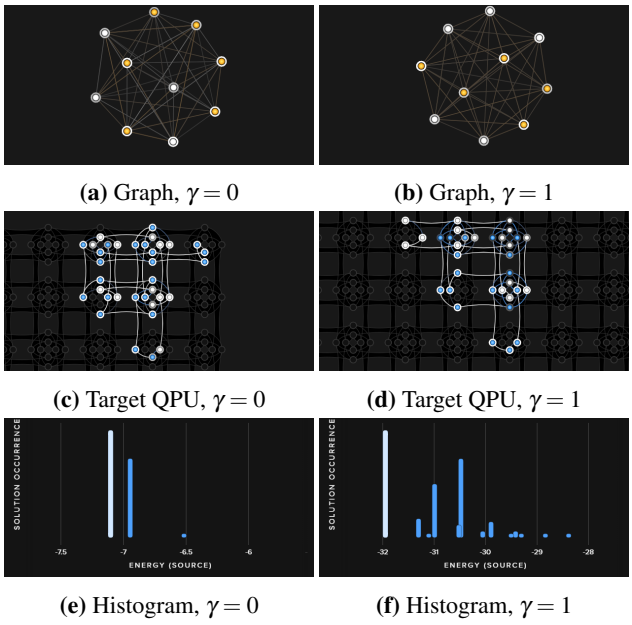

(a) Graph, $\gamma = 0$ **(b)** Graph, $\gamma = 1$

(c) Target QPU, $\gamma = 0$ **(d)** Target QPU, $\gamma = 1$

(e) Histogram, $\gamma = 0$ **(f)** Histogram, $\gamma = 1$

Figure 3 Upper row: graph representation of the optimization problem. Yellow dots denote a quantum variable in the state '1' while white dots mean state '0'. Middle row: actual mapping of the problem on the quantum computer hardware. Here, several physical qubits may be combined to form a single logical qubit. Lower row: Histogram of the measurement outcomes after 100 runs. The bright blue bars are the occurrences of the global optimum.

in Figs. 3a and 3b visualize the quadratic optimization problems, whereas Figs. 3c and 3d present the mapping of the respective graphs to the chimera architecture. Finally, in Figs. 3e and 3f the histograms of the readout are shown. As quantum computations are inherently probabilistic, repeated annealing cycles yield different outcomes. As expected, for $\gamma = 0$ the histogram is more concentrated around two of the three main minima, while in the second case the histogram is more spread out. The global optimum for the case $\gamma = 0$ is $|1101101001\rangle$ with an energy of -7.1 and for $\gamma = 1$ it is $|0101101001\rangle$ with an energy of -31.9.

3.2 MVDR Beamforming

Minimum distortionless response (MVDR) beamforming [21] is a technique, which has received much attention for instance in spaceborne array-fed reflector SAR systems [12, 13, 11, 16]. The array is operated in receive mode, such that internal and external thermal noise as well as interferences are minimized. At the same time all the array element signals shall be combined such that the gain in a certain direction is set to a specific value b - usually 1. Although the MVDR beamforming problem is solvable on any classical computer and even has an analytic solution, it shall serve as entry example which can be extended to more complicated optimization problems, containing for instance inequality constraints. Those kind of optimization problems may be hard to be solved for a global optimum on classical computers in reasonable time.

The MVDR optimization problem may be cast in the form

$$\text{minimize} \quad \sum_{ij} r_{ij} w_i w_j^* \,, \quad r_{ij}, w_i \in \mathbb{C} \,, \tag{11}$$

$$\text{subject to} \quad \sum_{i} w_i E_i = b \,, \quad b \in \mathbb{R} \,, \tag{12}$$

with (r_{ij}) describing the noise channel covariance matrix. In order to feed such a problem to a quantum annealer, some adaption is required. First, in the interpretation of minimizing energy functionals, the MVDR constraint needs to be cast in a quadratic form. Then, under the simplifying assumption $r_{ij} = \delta_{ij}$, the optimization problem writes

$$e_\mu = e'_\mu + \gamma e''_\mu = \sum_{i=0}^{N_\mathrm{c}-1} w_i w_i^* + \gamma \left| \sum_{i=0}^{N_\mathrm{c}-1} w_i E_i - b \right|^2 \,, \tag{13}$$

with N_c the number of array elements (or receive channels for that matter). A second difficulty is associated with the fact that a quantum annealer is a digital device and therefore cannot perform optimizations on a continuous Hilbert space. This means the complex variables w_i need to be modelled using binary qubits. For the purpose of solving linear systems of equations a real valued discrete variable model has been proposed for instance in [17]. In this context a discrete variable model could take the form

$$w_i = c \sum_{km} \mathrm{i}^m \left(2^k x_{ikm} - d\,\delta_{0k} \right) \,,$$

where N_b would denote the number of bits per real and imaginary part. The choice of the parameters b, c and d follows a heuristic, whereby the quantization of the coefficients w_i shall be matched to the field E_i. With this in mind, the following parameters have been utilized:

$$b = 1 \,, \tag{14}$$

$$c = \frac{\max\{|E'_0|, \ldots, |E'_{N_\mathrm{c}-1}|, |E''_0|, \ldots, |E''_{N_\mathrm{c}-1}|\}}{(2^{N_\mathrm{b}} - 1 - d) \sum_i |E_i|^2} \,, \tag{15}$$

$$d = \frac{1}{2} \left(2^{N_\mathrm{b}} - 1 \right) \,. \tag{16}$$

After some calculation, the energy functions may be expanded according to

$$e'_\mu = c^2 \sum_{ijklmn} 2^k \delta_{ij} \delta_{mn} \left(2^l - 2d\,\delta_{kl} \right) x_{ikm} x_{jln} + 2c^2 d^2 N_\mathrm{c} \tag{17}$$

and

$$\begin{aligned} e''_\mu = c^2 \sum_{ijklmn} 2^{k+1} \Big[& A_{ij} 2^{l-1} \delta_{mn} + B_{ij} 2^l \delta_{0m} \delta_{1n} \\ & - d \left(\sum_{j'} A_{ij'} + (-1)^m \sum_{j'} B_{ij'} \right) \delta_{ij} \delta_{kl} \delta_{mn} \\ & - b/c \left(E'_i \delta_{0m} - E''_i \delta_{1m} \right) \delta_{ij} \delta_{kl} \delta_{mn} \Big] x_{ikm} x_{jln} \\ & + 2c^2 d^2 \sum_{ij} (A_{ij} + B_{ij}) - 2bcd \sum_i (E''_i - E'_i) + b^2 \,, \end{aligned} \tag{18}$$

where $A_{ij} = E'_i E'_j + E''_i E''_j$ and $B_{ij} = E''_i E'_j - E'_i E''_j$.

In this MVDR beamforming example we consider a linear array comprising five elements. The complex weights w_i have been quantized using two times four bits. This amounts to 40 qubits, implying a solution Hilbert space with 2^{40} points. The regularization parameter γ has been set to one. Here again D-Waves' quantum annealer has been utilized, however, now addressing the next generation pegasus architecture Advantage 4.1 [3], employing 5760 qubits. The graph mapping on the quantum computer topology is shown in Fig. 4a. Here, already 201 physical qubits were required in order to construct the 40 logical qubits. Figure 4b presents a part of the histogram with

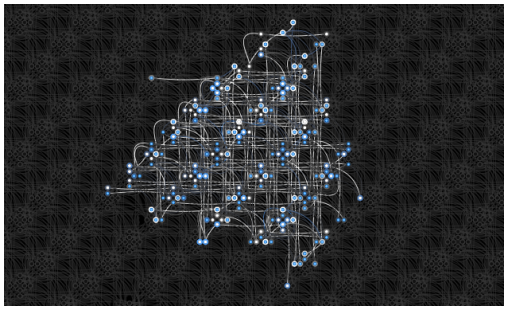

(a) Target QPU

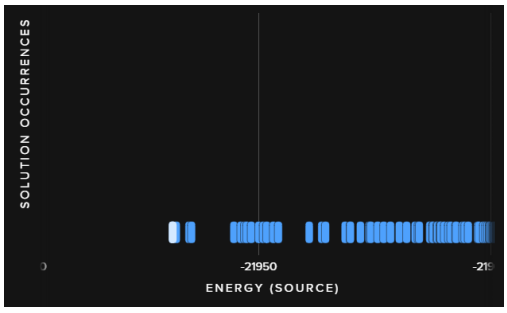

(b) Histogram

Figure 4 Eigenenergies for the sensor combinations.

1000 runs and 20 μs annealing time, where each solution

has been found only once. This is clearly a consequence of the size of the solution space and also of its topology with many local minima not too far away, in terms of the energy level, from the global optimum. The four best solutions, found by the quantum computer, are presented in Fig. 5. Here, the array gain patterns $G(\vartheta)$, with the main beam steered to an angle of 10°, have been plotted versus the coordinate ϑ. As reference for comparison, the analytic solution to the MVDR optimization problem is shown. The reason why the exact solution may have not been found could be (at least) threefold: First, by introducing the absolute squared in equation (13) the optimization problem has been altered, having potentially different solutions as the original problem (13). A second reason is that the quantization of the weights w_i uses a different model as for instance the floating point arithmetic of standard digital computers. And finally, as mentioned before, the size and topology of the solutions space as well as quantum noise might prevent the quantum computer converging to the ground state solution. Nevertheless, this example demonstrates that optimization problems with continuous variables are in principle solvable on a quantum computer.

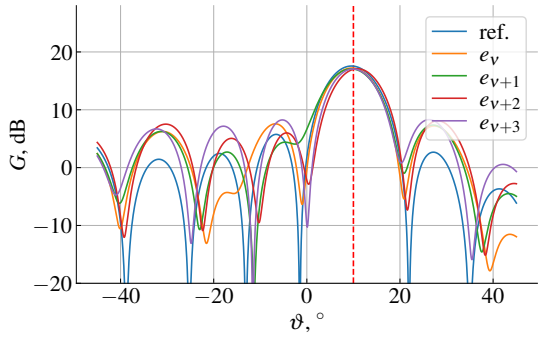

Figure 5 Array gain patterns versus angle ϑ. As reference the MVDR beam steered at 10° is shown. The solutions generated by the quantum computer may lie close to the global optimum e_0.

4 Conclusion

We have presented two dedicated optimization problems in array processing, which have been solved with the aid of D-Waves' quantum annealing system. The quantum nature of such devices allows, in principle, solving very high-dimensional problems. As a first example a sparse array problem has been solved on a first-generation quantum annealing system, showing promising results for a low number of qubits. As a second example the MVDR beamforming problem has been translated to a binary quadratic optimization problem and solved on a D-Waves' newer quantum computer architecture. It turns out that a limiting factor in the capability of finding a global optimum lies in the solution topology itself. But also the current state-of-the-art of quantum annealers have development potential, regarding for instance the number of fully entangled and error corrected qubits. Insofar the challenge of demonstrating quantum supremacy over classical computers remains not only in terms of algorithm execution speed but also in terms of problem size and complexity. However, the promising potential of quantum computation becomes more and more visible and progress on the hardware side as well as on the software side is just a question of time. In view of the numerous applications such as array processing, a leap forward in the utilization of quantum computers can be expected.

5 Literature

[1] D. Aharonov, W. van Dam, J. Kempe, Z. Landau, S. Lloyd, and O. Regev, "Adiabatic Quantum Computation is Equivalent to Standard Quantum Computation," *SIAM Review*, vol. 50, no. 4, pp. 755–787, 2008.

[2] T. Albash and D. A. Lidar, "Adiabatic Quantum Computation," *Reviews of Modern Physics*, vol. 90, Jan 2018.

[3] K. Boothby, P. Bunyk, J. Raymond, and A. Roy, "Next-Generation Topology of D-Wave Quantum Processors," arXiv:2003.00133v1 [quant-ph], Feb 2020.

[4] M. Born and V. Fock, "Beweis des Adiabatensatzes," *Zeitschrift für Physik*, vol. 51, no. 3-4, pp. 165–180, Mar 1928.

[5] P. I. Bunyk, E. M. Hoskinson, M. W. Johnson, E. Tolkacheva, F. Altomare, A. J. Berkley, R. Harris, J. P. Hilton, T. Lanting, A. J. Przybysz, and et al., "Architectural Considerations in the Design of a Superconducting Quantum Annealing Processor," *IEEE Transactions on Applied Superconductivity*, vol. 24, no. 4, pp. 1–10, Aug 2014.

[6] C. I. Coman, I. E. Lager, and L. P. Ligthart, "Design considerations in sparse array antennas," in *3rd European Radar Conference*, 2006, pp. 72–75.

[7] D-Wave Systems Inc., *Technical Description of the D-Wave Quantum Processing Unit*, May 2021, D-Wave User Manual 09-1109A-Y.

[8] D. de Falco and D. Tamascelli, "An introduction to quantum annealing," *RAIRO - Theoretical Informatics and Applications*, vol. 45, no. 1, pp. 99–116, Jan 2011.

[9] N. Goodman, S. C. Lin, D. Rajakrishna, and J. Stiles, "Processing of Multiple-Receiver Spaceborne Arrays for Wide-Area SAR," *IEEE Transactions on Geoscience and Remote Sensing*, vol. 40, no. 4, pp. 841–852, Apr 2002.

[10] R. Harris, M. W. Johnson, T. Lanting, A. J. Berkley, J. Johansson, P. Bunyk, E. Tolkacheva, E. Ladizinsky, N. Ladizinsky, T. Oh, and et al., "Experimental Investigation of an Eight-Qubit Unit Cell in a Superconducting Optimization Processor," *Physical Review B*, vol. 82, no. 2, Jul 2010.

[11] S. Huber, F. Q. de Almeida, M. Villano, M. Younis, G. Krieger, and A. Moreira, "Tandem-L: A Technical Perspective on Future Spaceborne SAR Sensors for Earth Observation," *IEEE Transactions on Geo-*

science and Remote Sensing, vol. 56, no. 8, pp. 4792–4807, Aug 2018.

[12] S. Huber, G. Krieger, and A. Moreira, "A Defocused and Cross-Pol-optimized Array-Fed Reflector Antenna Concept for Spaceborne SAR Applications," in *12th European Conference on Synthetic Aperture Radar (EUSAR)*, Jun 2018, pp. 1153–1157.

[13] G. Krieger, S. Huber, M. Younis, A. Moreira, J. Reimann, P. Klenk, M. Zink, M. Villano, and F. Q. de Almeida, "In-Orbit Relative Amplitude and Phase Antenna Pattern Calibration for Tandem-L," in *12th European Conference on Synthetic Aperture Radar (EUSAR)*, Jun 2018.

[14] M. Lavalle, I. Seker, J. Ragan, E. Loria, R. Ahmed, B. P. Hawkins, S. Prager, D. Clark, R. Beauchamp, M. Haynes, P. Focardi, N. Chahat, M. Anderson, K. Matsuka, V. Capuano, and S.-J. Chung, "Distributed Aperture Radar Tomographic Sensors (DARTS) to Map Surface Topography and Vegetation Structure," in *IEEE International Geoscience and Remote Sensing Symposium IGARSS*, 2021, pp. 1090–1093.

[15] A. Lucas, "Ising formulations of many NP problems," *Frontiers in Physics*, vol. 2, Feb 2014.

[16] A. Moreira, M. Bachmann, W. Balzer, D. B. Tridon, E. Diedrich, T. Fritz, C. Grigorov, R. Kahle, G. Krieger, I. Hajnsek, S. Huber, H. Jörg, P. Klenk, M. Lachaise, M. Maier, E. Maurer, K. Papathanassiou, A. Parizzi, P. Prats, J. Reimann, M. Rodriguez, B. Schättler, M. Schwinger, D. Schulze, U. Steinbrecher, M. Villano, M. Younis, F. De Zan, M. Zink, and M. Zonno, "Tandem-L: Project Status and Main Findings of the Phase Bl Study," in *IEEE International Geoscience and Remote Sensing Symposium (IGARSS)*, 2018, pp. 8667–8670.

[17] D. Ottaviani and A. Amendola, "Low Rank Non-Negative Matrix Factorization with D-Wave 2000Q," arXiv:1808.08721v1 [quant-ph], Aug 2018.

[18] A. Patwari, *Sparse Linear Antenna Arrays: A Review*, 2nd ed. IntechOpen, Sep 2021. [Online]. Available: https://www.intechopen.com/online-first/78401

[19] M. Rodrizuez-Cassola, N. Sakar, E. Rodrigues-Silva, J. Matar, P. M. N. Thi, L. Dell'Amore, M. Zonno, P. Prats-Iraola, G. Krieger, A. Moreira, and N. Gebert, "Multistatic SAR Constellations: An Opportunity for Scalable Systems with Single-Pass Interferometric Capabilities," in *IEEE International Geoscience and Remote Sensing Symposium IGARSS*, 2021, pp. 1085–1085.

[20] S. Tebaldini, L. Flora, and F. Rocca, "A Mimo Multi-Static SAR Satellite Formation for High Resolution 3D Imaging at Longer Wavelengths," in *IEEE International Geoscience and Remote Sensing Symposium IGARSS*, 2021, pp. 1086–1089.

[21] H. L. V. Trees, *Optimum Array Processing*. John Wiley & Sons, Inc., 2002.